

Birefringence and dichroism of the vacuum in the field of a standing electromagnetic wave

© I.A. Aleksandrov^{1,2}, D.V. Chubukov³, A.G. Tkachev¹, A.I. Klochaj¹

¹ St. Petersburg State University, St. Petersburg, Russia

² Ioffe Institute, St. Petersburg, Russia

³ ITMO University, St. Petersburg, Russia

e-mail: i.aleksandrov@spbu.ru

Received August 30, 2024

Revised August 30, 2024

Accepted September 16, 2024

Vacuum birefringence and dichroism are investigated in the setup involving a probe photon traversing a strong standing electromagnetic wave formed by two counterpropagating plane-wave laser beams. The analysis is based on the evaluation of the polarization tensor. We consider both the regime of relatively low laser frequency and photon energy and the domain where the energies are of the order of the electron rest energy. In the former case, if the external field is sufficiently weak, one can obtain very accurate predictions by means of the local values of the leading-order contribution to the Heisenberg-Euler effective Lagrangian. However, to address the high-energy and strong-field domains, one has to employ different methods. Here we utilize the locally-constant field approximation (LCFA) and compute the real and imaginary parts of the polarization tensor varying the propagation direction of the probe photon. It is demonstrated that if the propagation axis of the photon is parallel to that of the laser beams, then the effects are governed entirely by the counterpropagating beam, while the copropagating one is irrelevant. If the photon travels perpendicularly to the laser beam axis, the two plane waves are equally significant. In this case, within the Heisenberg-Euler approximation, it is sufficient to multiply the corresponding single-wave result by a factor of two, whereas the LCFA predictions are less trivial as they incorporate the higher-order nonlinear contributions.

Keywords: vacuum birefringence, dichroism, quantum electrodynamics, strong fields, nonlinear effects.

DOI: 10.61011/EOS.2024.09.60045.7009-24

1. Introduction

According to quantum electrodynamics (QED), the physical vacuum state cannot be reviewed as a trivial void space because of vacuum fluctuations which manifest themselves, e.g., as some non-linear phenomena occurring in the external electromagnetic fields. Classical Maxwell theory is added with quantum corrections leading to non-trivial polarization properties of vacuum [1–8] and to the effects of vacuum birefringence and dichroism. In this study, we investigate these phenomena in a superposition of two opposing laser beams forming a standing electromagnetic wave.

From the experimental standpoint, in the laser low-frequency mode and at low frequencies of the probe photon (compared with the rest energy of the electron divided by the reduced Planck constant), we may try to use the high-precision experimental methods in the relevant area [9–19]. To obtain the exact theoretical predictions in such a mode it is enough to review only external field as a locally constant field and use the confined expression for the efficient Heisenberg-Euler Lagrangian. If the external field is relatively low, we can consider only the higher-order quantum correction included in the effective Lagrangian [20]. If the external field is high, so that the Heisenberg-Euler approximation is no longer valid in the leading order, then a computation can be made based on the

local values of the polarization operator obtained in constant crossed fields [21–25]. Such nonperturbative approach is called a locally-constant field approximation (LCFA). It turned out that LCFA also allows partially investigate the domain of high laser frequencies and high-energy probe photons [26]. From an experimental point of view, this mode may also prove to be very promising, since generally it corresponds to higher values of the signal [25,27,28]. Moreover, LCFA also predicts non-zero imaginary part of the polarization operator, and, thus, allows for the vacuum dichroism effect. According to the optical theorem, the imaginary part determines the total probability of the photon disintegration into an electron-positron pair, which can be considered as a probability of photon absorption. If this value depends on the polarization of the probe photon, then, the quantum vacuum exhibits dichroic properties in the presence of an appropriate electromagnetic background.

In this study we will use both, LCFA and Heisenberg-Euler approximation to study the vacuum birefringence and dichroism phenomena in the field of standing electromagnetic wave. Our aim — is to compare two theoretical approaches in a wide range of the field parameters for various energy (frequency) values of the probe photon. To obtain new information about the nonlinear effects under consideration, we will also change the direction of photon propagation and compare the standing wave with a scenario where only one plane electromagnetic wave is included.

This study is structured as follows. Section 2 outlines the task in whole. In Section 3 it is discussed how to study the vacuum birefringence using the efficient Heisenberg-Euler Lagrangian. In Section 4 the LCFA-based approximation method is formulated. Section 5 contains the results of our computations. In Section 6 conclusions are provided.

In the article we use the following units of measurement $\hbar = c = 1$, $\alpha = e^2/(4\pi)$ (α — fine structure constant), $e < 0$.

2. Parameters of external field and probe photon

The task setting includes a probe photon with an energy $q^0 = q_0$ and a standing electromagnetic wave expressed as a vector potential of the following kind:

$$\mathcal{A}(t, z) = \frac{\mathcal{E}_0}{\omega} \sin \omega t \cos \omega z \mathbf{e}_x, \quad (1)$$

where ω — wave frequency, \mathcal{E}_0 — field strength amplitude, and the unit vectors along the Cartesian axes are denoted as $\{\mathbf{e}_i\}$ ($\mathbf{x} = x\mathbf{e}_x + y\mathbf{e}_y + z\mathbf{e}_z$). Scalar potential \mathcal{A}_0 is equal to zero. Vector potential (1) corresponds to the following expressions for the components of electric and magnetic fields:

$$\mathbf{E}(t, z) = -(\partial_t \mathcal{A}_x) \mathbf{e}_x = -\mathcal{E}_0 \cos \omega t \cos \omega z \mathbf{e}_x, \quad (2)$$

$$\mathbf{B}(t, z) = (\partial_z \mathcal{A}_x) \mathbf{e}_y = -\mathcal{E}_0 \sin \omega t \sin \omega z \mathbf{e}_y. \quad (3)$$

A standing electromagnetic wave is formed by two counter linearly polarized laser beams propagating along the z axis:

$$\mathcal{A}(t, z) = \frac{(\mathcal{E}_0/2)}{\omega} [\sin \omega(t+z) + \sin \omega(t-z)] \mathbf{e}_x. \quad (4)$$

In the task under consideration, there are no constant components of the electromagnetic field (the possibility of experimental observation of birefringence in a magnetic field has been studied, for example, in papers [29,30]).

The probe photon is propagating in an arbitrary direction defined by angles θ and φ , i.e. 4-momentum q^μ is selected as $q^\mu = q_0 (1, \sin \theta \cos \varphi, \sin \theta \sin \varphi, \cos \theta)^t$. Let us designate the final 4-pulse of photon as k^μ .

Later, it will be convenient to use the following dimensionless parameters:

$$\xi = \frac{|e\mathcal{E}_0|}{m\omega}, \quad \chi_0 = \frac{|e\mathcal{E}_0|q^0}{m^3}. \quad (5)$$

The first parameter is called the relativistic field amplitude parameter (it is also often referred to as a_0). If $\xi \gtrsim 1$, then, the external field accelerates the electrons to the relativistic energies. Planck constant is not included in the expression ξ . The second parameter in (5) — is the so-called parameter of quantum nonlinearity which plays central role in the analysis of QED-effects in strong external fields (it is proportionate to \hbar).

In the leading order for the fine structure constant α effects of vacuum birefringence and dichroism are observed in Feynman diagram shown in Fig. 1. The initial and final states of the photon (wavy lines) may differ due to the presence of a vacuum loop containing electronic Green's functions in a given external field. In the right part of the Figure the high-order contributions for the external field strength \mathcal{E}_0 are shown. These terms will be calculated approximately using an approach based on the use of one-loop effective Heisenberg-Euler Lagrangian. The diagram on the left side will be calculated by locally constant field approximation (LCFA).

In accordance with Feynman rules in QED, the amplitude corresponding to the diagram on the left side of Fig.1 can generally be represented as

$$\mathcal{S}(q, k) = \frac{i}{\sqrt{4q_0k_0}} \varepsilon_\mu(q) \Pi^{\mu\nu}(q, k) \varepsilon_\nu^*(k), \quad (6)$$

where $\Pi^{\mu\nu}$ — polarization tensor in the external field, and $\varepsilon_\mu(q)$ and $\varepsilon_\nu(k)$ — 4-vectors of polarization standing for the initial and final states of the photon, respectively. We will discuss only the field-dependent part of this tensor, which describes the effects under consideration. Despite the fact that a fermionic loop in the Feynman diagram can lead to a nonzero transfer of the energy-momentum, i.e. k^μ may differ from q^μ , and further we will focus on the elastic process ($k = q$), that corresponds to the birefringence and dichroism phenomena.

3. Heisenberg-Euler approximation in the leading order

In this section, we will consider an approach based on the perturbative expansion of the polarization tensor over the field strength. It can be derived from a single-loop effective Lagrangian in the presence of a constant electromagnetic field (see [20]). Three Feynman diagrams shown on the right side of Fig. 1 can be approximately calculated using a closed expression for the corresponding Lagrangian of the leading order. Within the framework of this approach, the polarization tensor can be represented as follows [20]:

$$\Pi_{\text{HE}}^{\mu\nu}(q, k) = \frac{\alpha}{45\pi} \frac{e^2}{m^4} \int d^4x e^{i(k-q)x} \times [4(qF)^\mu(kF)^\nu + 7(qG)^\mu(kG)^\nu], \quad (7)$$

where $x = (t, \mathbf{x})$, $(kF)^\mu \equiv k_\lambda F^{\lambda\mu}$, while tensors $F^{\mu\nu}$ and $G^{\mu\nu}$ depend on x . Here we use standard expression for the electromagnetic tensor, $F_{\mu\nu} = \partial_\mu \mathcal{A}_\nu - \partial_\nu \mathcal{A}_\mu$. Dual tensor is defined as $G_{\mu\nu} = (1/2)\epsilon_{\mu\nu\lambda\sigma} F^{\lambda\sigma}$, where $\epsilon_{\mu\nu\lambda\sigma}$ — Levi-Civita tensor. Calculating the integral in the equation (7) leads to conservation laws that change the momentum and energy of the photon by $\pm 2\omega$ or leave them unchanged. Since only elastic scattering is of interest to us, we will save only those terms that contain $\delta^{(4)}(k - q)$. We may directly get

$$\Pi_{\text{HE, elastic}}^{\mu\nu}(q, k) = \frac{16\pi^3 \alpha}{45} m^2 \chi_0^2 \delta^{(4)}(k - q) \mathcal{P}_{\text{HE}}^{\mu\nu}, \quad (8)$$

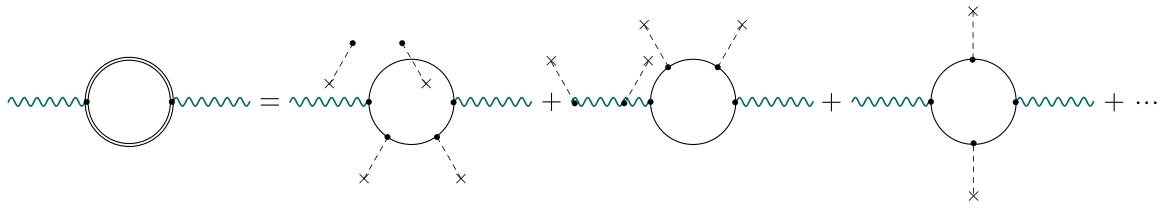


Figure 1. Feynman diagram describing the effects of vacuum dichroism and birefringence, and its expansion with respect to the external field strength. Zero order contribution is neglected. Double lines correspond to the electronic Green functions in the external field, single lines — to propagators of free electrons, wavy lines — to the initial and final photon, and vertices with crosses — to interaction with the external classical field.

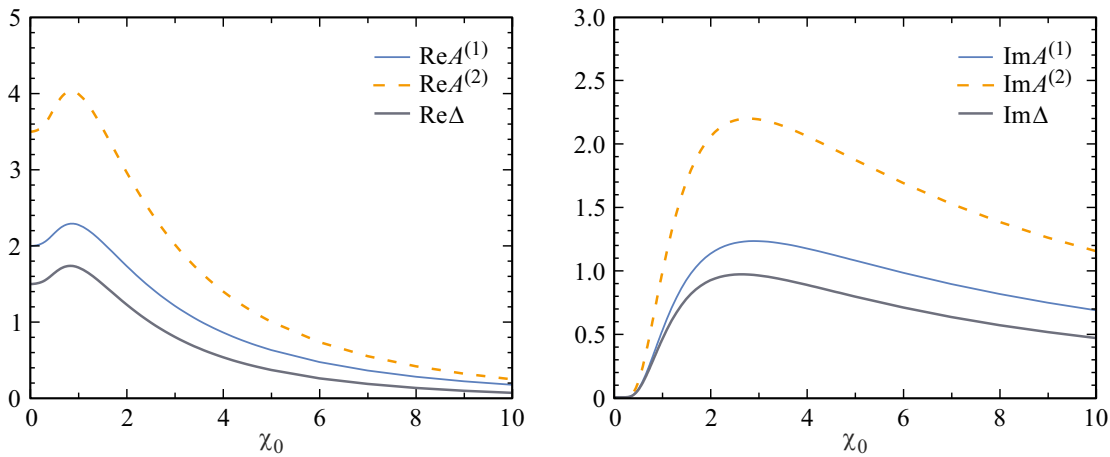


Figure 2. The real and imaginary parts of dimensionless values $A^{(1)}$, $A^{(2)}$ and Δ , calculated within LCFA depending on the quantum parameter of nonlinearity χ_0 in case of $\theta = \varphi = 0$. According to formulae (12)–(14), Heisenberg-Euler approximation gives $A_{HE}^{(1)} = 2$, $A_{HE}^{(2)} = 7/2$ and $\Delta_{HE} = 3/2$ irrespective of χ_0 .

$$\mathcal{P}_{HE}^{\mu\nu} = \begin{pmatrix} \sin^2 \theta & & & & \\ \times \left(1 + \frac{3}{4} \sin^2 \varphi\right) & \sin \theta \cos \varphi & \frac{7}{4} \sin \theta \sin \varphi & & 0 \\ \sin \theta \cos \varphi & 1 + \cos^2 \theta & 0 & & -\frac{1}{2} \sin 2\theta \cos \varphi \\ \frac{7}{4} \sin \theta \sin \varphi & 0 & \frac{7}{4} (1 + \cos^2 \theta) & & -\frac{7}{8} \sin 2\theta \sin \varphi \\ 0 & -\frac{1}{2} \sin 2\theta \cos \varphi & -\frac{7}{8} \sin 2\theta \sin \varphi & & \sin^2 \theta \\ & & & & \times \left(1 + \frac{3}{4} \sin^2 \varphi\right) \end{pmatrix}. \quad (9)$$

Physically observed quantities are determined by the amplitude of the process (6). To study the effect of vacuum birefringence we need to compute a non-zero difference of two amplitudes for the two perpendicular 4-vectors of polarization $\varepsilon_\mu^{(w)}$ ($w = 1, 2$) of the probe photon. Let us introduce

$$\varepsilon_\mu^{(1)} = (0, \cos \theta \cos \varphi, \cos \theta \sin \varphi, -\sin \theta)^t, \quad (10)$$

$$\varepsilon_\mu^{(2)} = (0, -\sin \varphi, \cos \varphi, 0)^t. \quad (11)$$

The amplitude (6) is proportional to $\varepsilon_\mu(q) \mathcal{P}^{\mu\nu} \varepsilon_\nu^*(k)$, so we will discuss our results further in terms of the following quantities:

$$A_{HE}^{(1)} = \varepsilon_\mu^{(1)} \mathcal{P}_{HE}^{\mu\nu} \varepsilon_\nu^{(1)} = (1 + \cos^2 \theta) \left(1 + \frac{3}{4} \sin^2 \varphi\right), \quad (12)$$

$$A_{HE}^{(2)} = \varepsilon_\mu^{(2)} \mathcal{P}_{HE}^{\mu\nu} \varepsilon_\nu^{(2)} = (1 + \cos^2 \theta) \left(1 + \frac{3}{4} \cos^2 \varphi\right). \quad (13)$$

We see that the dependencies on θ and φ are factorized. The difference is written as

$$\Delta_{HE} \equiv A_{HE}^{(2)} - A_{HE}^{(1)} = \frac{3}{4} (1 + \cos^2 \theta) \cos 2\varphi. \quad (14)$$

It follows from this expression that, in the Heisenberg-Euler approximation, the birefringence of the vacuum in a standing wave is maximal if the probe photon propagates along or against the direction z . The effect fades away, if the probe photon is propagating along the bisecting lines of plane xy ($\varphi = \pi/4 + \pi n/2$).

Further, we will also compare our results for a standing wave with the results obtained when taking into account only the first term in equation (4). This corresponds to the plane wave propagating along the negative direction of axis z . In case $\theta = \varphi = 0$ see the results, e.g., in paper [26]. For arbitrary angles the polarization tensor is written as

$$\Pi_{HE, PW, elastic}^{\mu\nu}(q, k) = \frac{16\pi^3 \alpha}{45} m^2 \chi_0^2 \delta^{(4)}(k - q) \mathcal{P}_{HE, PW}^{\mu\nu}, \quad (15)$$

$$\mathcal{P}_{\text{HE, PW}}^{\mu\nu} = \begin{pmatrix} \frac{1}{2} \sin^2 \theta \left(1 + \frac{3}{4} \sin^2 \varphi\right) & \frac{1}{2} \sin \theta \cos \varphi (1 + \cos \theta) & \frac{7}{8} \sin \theta \sin \varphi (1 + \cos \theta) & \frac{1}{2} \sin^2 \theta \left(\frac{3}{4} \sin^2 \varphi - 1\right) \\ \frac{1}{2} \sin \theta \cos \varphi (1 + \cos \theta) & 2 \cos^4 \theta / 2 & 0 & -\frac{1}{2} \sin \theta \cos \varphi (1 + \cos \theta) \\ \frac{7}{8} \sin \theta \sin \varphi (1 + \cos \theta) & 0 & \frac{7}{2} \cos^4 \theta / 2 & -\frac{7}{8} \sin \theta \sin \varphi (1 + \cos \theta) \\ \frac{1}{2} \sin^2 \theta \left(\frac{3}{4} \sin^2 \varphi - 1\right) & -\frac{1}{2} \sin \theta \cos \varphi (1 + \cos \theta) & -\frac{7}{8} \sin \theta \sin \varphi (1 + \cos \theta) & \frac{1}{2} \sin^2 \theta \left(1 + \frac{3}{4} \sin^2 \varphi\right) \end{pmatrix}. \quad (16)$$

Here

$$A_{\text{HE, PW}}^{(1)} = \frac{1}{2} (1 + \cos \theta)^2 \left(1 + \frac{3}{4} \sin^2 \varphi\right), \quad (17)$$

$$A_{\text{HE, PW}}^{(2)} = \frac{1}{2} (1 + \cos \theta)^2 \left(1 + \frac{3}{4} \cos^2 \varphi\right). \quad (18)$$

$$\Delta_{\text{HE, PW}} \equiv A_{\text{HE, PW}}^{(2)} - A_{\text{HE, PW}}^{(1)} = \frac{3}{8} (1 + \cos \theta)^2 \cos 2\varphi. \quad (19)$$

When $\theta = 0$ the results for the plane wave coincide with results obtained for the standing wave (12)–(14).

4. Locally constant field approximation (LCFA)

It turns out that when considering the external field as locally constant, higher-order contributions in field strength can be taken into account by estimating the diagram on the left side of Fig. 1, i.e. without using the perturbative expansion on the right side. For this purpose, we may use the expression for the polarization tensor obtained in the case of constant crossed fields [21–23], and then integrate it over x , using real spatiotemporal dependence of the external field [24]. For our case the contribution of the elastic process is expressed as

$$\Pi_{\text{LCFA, elastic}}^{\mu\nu}(q, k) = \frac{16\pi^3 \alpha}{3} m^2 \delta^{(4)}(k - q) \times \langle \chi^{2/3} \{ (A - B) \mathcal{F}^{\mu\nu} + (A + 2B) \mathcal{G}^{\mu\nu} \} \rangle_{t,z}, \quad (20)$$

where

$$\chi = \frac{|e| \sqrt{-(kF)^2}}{m^3} \quad (21)$$

represents a local value of the quantum parameter of nonlinearity $[(kF)^2 \equiv (kF)^\mu (kF)_\mu]$. In formula (20) we also use the following definitions:

$$\mathcal{F}^{\mu\nu} = \frac{(kF)^\mu (kF)^\nu}{(kF)^2}, \quad \mathcal{G}^{\mu\nu} = \frac{(kG)^\mu (kG)^\nu}{(kG)^2}, \quad (22)$$

$$A = \int_{-1}^1 dv w^{1/3} f'(u), \quad B = \int_{-1}^1 dv w^{-2/3} f'(u), \quad (23)$$

$$w = \frac{4}{1 - v^2}, \quad u = \left(\frac{w}{\chi}\right)^{2/3}, \quad (24)$$

$$f(u) = i \int_0^\infty d\tau e^{-i(u\tau + \tau^3/3)} = \pi \text{Gi}(u) + i\pi \text{Ai}(u). \quad (25)$$

Here $\text{Gi}(u)$ and $\text{Ai}(u)$ — Scorer's [31] and Airy functions, respectively. The value of parameter χ is varied in space and with time and defined by local values of the external field $F^{\mu\nu}$. Correspondingly, u also depends on time t and spatial coordinate z . Average value over t and z in expression (20) (angle-brackets) demonstrates that the results shall be averaged in terms of temporal and spatial period of standing wave. It follows from classical expression $z(t) = z_0 + t \cos \theta$ for „photon trajectory“, where we have to make averaging over z_0 and t . A simple replacement of variables with transition from z_0 to z leads to the technique described above.

If the local values of χ are small, then the following asymptotic expansions can be used:

$$A = -\chi^{4/3} \left[\frac{1}{3} + \frac{4}{35} \chi^2 + \frac{20}{99} \chi^4 + \mathcal{O}(\chi^6) \right] - \frac{i\pi}{2} \sqrt{\frac{3}{2}} \chi^{1/3} e^{-8/(3\chi)} [1 + \mathcal{O}(\chi)], \quad (26)$$

$$B = -\chi^{4/3} \left[\frac{1}{15} + \frac{8}{315} \chi^2 + \frac{20}{429} \chi^4 + \mathcal{O}(\chi^6) \right] - \frac{i\pi}{8} \sqrt{\frac{3}{2}} \chi^{1/3} e^{-8/(3\chi)} [1 + \mathcal{O}(\chi)]. \quad (27)$$

We see that the imaginary part of the polarization tensor is strongly suppressed in $\chi \ll 1$ regime. Expanding the expression (20), we find that the higher-order contribution exactly coincides with the Heisenberg-Euler approximation (8), (9).

We also mention that local approximations in various forms can be used to describe other QED phenomena in high fields. For example, Sauter-Schwinger effect associated with the vacuum generation of electron-positron pairs can be investigated using LCFA [32–41].

5. Numerical results

Lets start our numerical analysis with the most simple case $\theta = \varphi = 0$, corresponding to the probe photon propagating along the axis z and polarized either along direction x ($\varepsilon^{(1)}$), or along y ($\varepsilon^{(2)}$). First, as mentioned above, in the Heisenberg-Euler approximation, the result for a standing wave (9) is exactly equal to the expression for a plane wave (16), allowing for the amplitudes \mathcal{E}_0 and $\mathcal{E}_0/2$ selected respectively for these two scenarios. This means that the second term in equation (4) is absolutely non-essential, i.e. the properties of the probe photon are in no way affected by the associated laser pulse. Moreover, this is also true for LCFA. Fig. 2 illustrates the real and imaginary parts

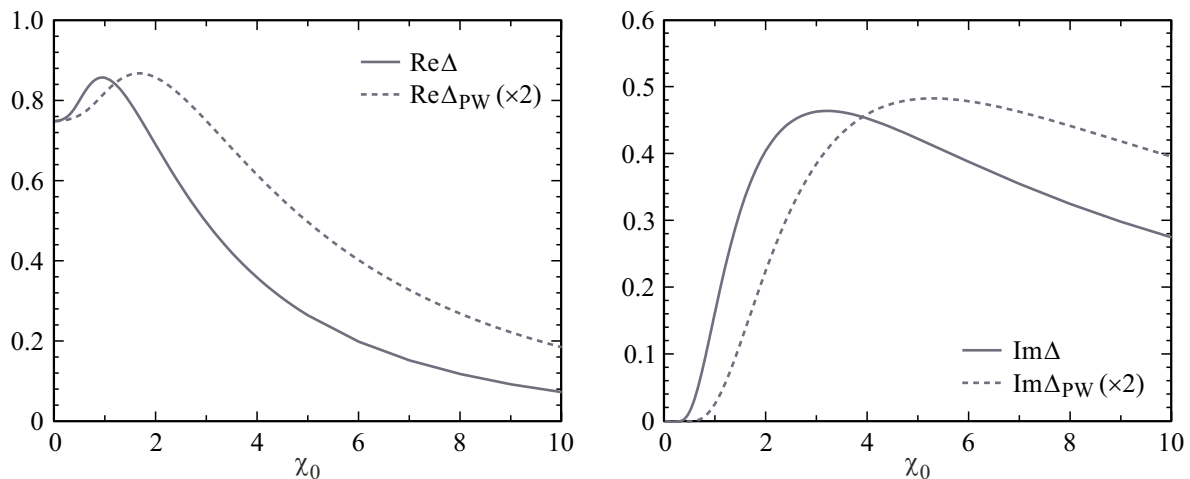


Figure 3. The real and imaginary parts of the difference Δ computed within LCFA in the standing wave field (1) and in the field of a single plane wave, propagating in the negative direction of the axis z . Values for the plane wave are multiplied by a coefficient of 2. The probe photon is moving along the axis x ($\theta = \pi/2$, $\varphi = 0$).

of values $A^{(1)}$, $A^{(2)}$ and Δ as functions χ_0 . In the case of a plane-wave field, our numerical results turned out to be exactly the same as those obtained for the standing wave (1). Secondly, as seen from Fig. 2, it is clear that the Heisenberg-Euler approximation is accurate only in the area of small χ_0 ; for $\chi_0 = 0.5$ the real part Δ_{HE} differs from LCFA Δ prediction by 9%. The imaginary part is zero in the leading order, therefore, to describe the effect of vacuum dichroism, the contributions of higher orders, for example, via LCFA (20), shall be taken into account.

Lets consider non-zero angles θ and φ in the mode of low-field (low energies) $\chi_0 \ll 1$. Now the expression for a plane wave (16) and the result for a standing wave (9) do not match, since both terms in the equation (4) give non-zero contributions. For example, as θ increases, the birefringence signals (14) and (19) begin to differ notably from each other. For $\theta = \pi/2$ the expressions for a standing wave (12)–(14) are twice as much as the results for a plane wave (17)–(19).

To make the analysis with the derivatives χ_0 , lets plot a curve of Δ versus χ_0 for $\theta = \pi/2$, $\varphi = 0$, which corresponds to the probe photon moving along the axis x (Fig. 3). The results obtained for the plane wave scenario shall be multiplied by a factor of 2. While for $\chi_0 \ll 1$ the configuration with one plane wave is equivalent to the standing wave (1), for large χ_0 this is not true. This suggests that since the process is nonlinear, the effect of two identical plane waves in equation (4) does not match the result for one wave multiplied simply by a factor of 2. In the leading order, the elastic process under consideration involves absorption and emission of the same photon. This is either the quantum of the first laser beam or the quantum of the second beam. This means that the two plane waves act independently, which is not observed in higher-order contributions involving several acts of emission and absorption. LCFA approximation includes all these members and unambiguously indicates their significance

in the mode $\chi_0 \gtrsim 1$. We emphasize once again that the imaginary part is always absent in the higher terms as illustrated in Fig. 1. Finally, lets stress that, in order to quantify the effects of vacuum birefringence and dichroism, the pre-factor in (8) should be taken into account, which contains χ_0^2 .

Since Heisenberg-Euler approximation in the leading order represents the limit of small χ_0 in LCFA, it is reasonable to use it for describing vacuum birefringence if LCFA itself and $\chi_0 \ll 1$ are valid, as can be seen from the analytical expressions and our numerical examples. Although LCFA is inherently nonperturbative with respect to the classical field, it is still an approximate method, since in the framework of LCFA it is assumed that external field can be considered as locally constant and locally crossed. The precision of LCFA, apparently depends on ω , \mathcal{E}_0 and energy of the probe photon k^0 . Thus, according to [26], for instance, in case of the plane-wave field the application of LCFA is justified, if ξ significantly exceeds χ_0 , which in practice stands for $\xi \gg 1$ or $\chi_0 \ll \xi \lesssim 1$.

6. Conclusion

In this paper, the polarization tensor in the field of a standing electromagnetic wave was calculated using the locally constant field approximation (LCFA) and the Heisenberg-Euler approximation. The real and imaginary parts of this tensor stand, respectively, for vacuum birefringence and dichroism. It was demonstrated that for small values of the quantum parameter of nonlinearity ($\chi_0 \ll 1$), the latter approach gives accurate and simple predictions: the real part of the polarization tensor trivially depends on χ_0 and can be easily associated with the results for a single laser beam (for example, in case of transverse propagation, the obtained value should just be multiplied by 2). If the condition $\chi_0 \ll 1$ is not fulfilled anymore,

then it is necessary to go beyond the Heisenberg-Euler approximation. In this case, taking into account higher-order contributions by LCFA, we obtain a nontrivial dependence of both the real and imaginary parts on parameter χ_0 . The results obtained for a standing wave start to differ fundamentally from the computations in case of a single plane-wave beam.

Since a standing electromagnetic wave is featuring a much more intriguing configuration than a plane wave, it is advisable to compare local approximations with accurate results for this case. This issue is a critical line of our further research.

Funding

The study was performed with the financial support from the Russian Science Foundation (RSF) within the project No 23-72-01068.

Conflict of interest

The authors declare that they have no conflict of interest.

References

- [1] H. Euler, B. Kockel, *Naturwiss.*, **23**, 246 (1935).
- [2] W. Heisenberg, H. Euler, *Z. Phys.*, **98**, 714 (1936).
- [3] J. Schwinger, *Phys. Rev.*, **82**, 664 (1951). DOI: 10.1103/PhysRev.82.664
- [4] J.S. Toll, Ph.D. thesis, Princeton Univ., 1952.
- [5] R. Baier, P. Breitenlohner, *Acta Phys. Austriaca*, **25**, 212 (1967).
- [6] R. Baier, P. Breitenlohner, *Nuovo Cimento B*, **47**, 117 (1967). DOI: 10.1007/BF02712312
- [7] V.N. Bayer, A.I. Milstein, V.M. Strakhovenko, *ZhETF*, **69**, 1893 (1975) (in Russian).
- [8] W. Becker, H. Mitter, *J. Phys. A*, **8**, 1638 (1975). DOI: 10.1088/0305-4470/8/10/017
- [9] E.B. Aleksandrov, A.A. Anselm, A.N. Moskalev, *ZhETF*, **89**, 1181 (1985) (in Russian).
- [10] A. Di Piazza, K.Z. Hatsagortsyan, C.H. Keitel, *Phys. Rev. Lett.*, **97**, 083603 (2006). DOI: 10.1103/PhysRevLett.97.083603
- [11] T. Heinzl, B. Liesfeld, K.U. Amthor, H. Schwoerer, R. Sauerbrey, A. Wipf, *Opt. Commun.*, **267**, 318 (2006). DOI: 10.1016/j.optcom.2006.06.053
- [12] V. Dinu, T. Heinzl, A. Ilderton, M. Marklund, G. Torgrimsson, *Phys. Rev. D*, **89**, 125003 (2014). DOI: 10.1103/PhysRevD.89.125003
- [13] F. Karbstein, E.A. Mosman, *Phys. Rev. D*, **101**, 113002 (2020). DOI: 10.1103/PhysRevD.101.113002
- [14] F. Karbstein, *Annalen Phys.*, **534**, 2100137 (2022). DOI: 10.1002/andp.202100137
- [15] F. Karbstein, H. Gies, M. Reuter, M. Zepf, *Phys. Rev. D*, **92**, 071301(R) (2015). DOI: 10.1103/PhysRevD.92.071301
- [16] H.-P. Schlenvoigt, T. Heinzl, U. Schramm, T.E. Cowan, R. Sauerbrey, *Phys. Scr.*, **91**, 023010 (2016). DOI: 10.1088/0031-8949/91/2/023010
- [17] N. Ahmadinia, T.E. Cowan, R. Sauerbrey, U. Schramm, H.-P. Schlenvoigt, R. Schützhold, *Phys. Rev. D*, **101**, 116019 (2020). DOI: 10.1103/PhysRevD.101.116019
- [18] F. Karbstein, D. Ullmann, E.A. Mosman, M. Zepf, *Phys. Rev. Lett.*, **129**, 061802 (2022). DOI: 10.1103/PhysRevLett.129.061802
- [19] N. Ahmadinia, T. E. Cowan, J. Grenzer, S. Franchino-Viñas, A. Laso Garcia, M. Šmíd, T. Toncian, M.A. Trejo, R. Schützhold, *Phys. Rev. D*, **108**, 076005 (2023). DOI: 10.1103/PhysRevD.108.076005
- [20] F. Karbstein, R. Shaisultanov, *Phys. Rev. D*, **91**, 085027 (2015). DOI: 10.1103/PhysRevD.91.085027
- [21] I.A. Batalin, A.E. Shabad, *Prepr. FIAN*, **166** (1968) (in Russian).
- [22] N.B. Narozhny, *ZhETF*, **55**, 714 (1968) (in Russian).
- [23] V.I. Ritus, *Ann. Phys.*, **69**, 555 (1972). DOI: 10.1016/0003-4916(72)90191-1
- [24] S. Meuren, C.H. Keitel, A. Di Piazza, *Phys. Rev. D*, **88**, 013007 (2013). DOI: 10.1103/PhysRevD.88.013007
- [25] S. Bragin, S. Meuren, C.H. Keitel, A. Di Piazza, *Phys. Rev. Lett.*, **119**, 250403 (2017). DOI: 10.1103/PhysRevLett.119.250403
- [26] I.A. Aleksandrov, V.M. Shabaev, *Journ.Exp.Theor.Phys.*, **166**, 182 (2024) (in Russian). DOI: 10.31857/S0044451024080042
- [27] B. King, N. Elkina, *Phys. Rev. A*, **94**, 062102 (2016). DOI: 10.1103/PhysRevA.94.062102
- [28] Y. Nakamiya, K. Homma, *Phys. Rev. D*, **96**, 053002 (2017). DOI: 10.1103/PhysRevD.96.053002
- [29] F. Della Valle, A. Ejlli, U. Gastaldi, G. Messineo, E. Milotti, R. Pengo, G. Ruoso, G. Zavattini, *Eur. Phys. J. C*, **76**, 24 (2016). DOI: 10.1140/epjc/s10052-015-3869-8
- [30] G. Zavattini, F. Della Valle, A. Ejlli, G. Ruoso, *Eur. Phys. J. C*, **76**, 294 (2016). DOI: 10.1140/epjc/s10052-016-4139-0
- [31] R.S. Scorer, *Q. J. Mech. Appl. Math.*, **3**, 107 (1950). DOI: 10.1093/qjmam/3.1.107
- [32] N.B. Narozhny, S.S. Bulanov, V.D. Moor, V.S. Popov, *Pisma v ZhETF*, **80**, 434 (2004) (in Russian). DOI: 10.1134/1.1830652
- [33] S.S. Bulanov, N.B. Narozhny, V.D. Moor, V.S. Popov, *ZhETF*, **129**, 14 (2006) (in Russian).
- [34] F. Hebenstreit, R. Alkofer, H. Gies, *Phys. Rev. D*, **78**, 061701(R) (2008). DOI: 10.1103/PhysRevD.78.061701
- [35] S.S. Bulanov, V.D. Mur, N.B. Narozhny, J. Nees, V.S. Popov, *Phys. Rev. Lett.*, **104**, 220404 (2010). DOI: 10.1103/PhysRevLett.104.220404
- [36] S.P. Gavrilov, D.M. Gitman, *Phys. Rev. D*, **95**, 076013 (2017). DOI: 10.1103/PhysRevD.95.076013
- [37] I.A. Aleksandrov, G. Plunien, V.M. Shabaev, *Phys. Rev. D*, **99**, 016020 (2019). DOI: 10.1103/PhysRevD.99.016020
- [38] D.G. Sevostyanov, I.A. Aleksandrov, G. Plunien, V.M. Shabaev, *Phys. Rev. D*, **104**, 076014 (2021). DOI: 10.1103/PhysRevD.104.076014
- [39] I.A. Aleksandrov, D.G. Sevostyanov, V.M. Shabaev, *Symmetry*, **14**, 2444 (2022). DOI: 10.3390/sym14112444
- [40] I.A. Aleksandrov, D.G. Sevostyanov, V.M. Shabaev, *Phys. Rev. D*, **111**, 016010 (2025). DOI: 10.1103/PhysRevD.111.016010
- [41] A.G. Tkachev, I.A. Aleksandrov, V.M. Shabaev, arXiv:2408.04084.

Translated by EgoTranslating